# New Observational Capabilities for Studying the Lower Ionosphere using ISR

Michael J. Nicolls

CEDAR, 29 June 2009

SRI International

# Acknowledgements

Craig Heinselman, John Kelly - SRI International
Mike Kelley, Dave Hysell, and Don Farley - Cornell University
Sixto González, Nestor Aponte, and Mike Sulzer - Arecibo Observatory
Jorge Chau - Jicamarca Radio Observatory
Diego Janches, Dave Fritts, Sharon Vadas - NwRA / CoRA Division
Bob Robinson and Rich Behnke - NSF

# Outline

# Outline

1. Incoherent Scatter - Recent Advances (My Bias)
   - Theoretical Advances
   - Experimental Advances
   - Observational Advances
2. Incoherent Scatter from the *D* Region: Observations with PFISR
   - Past Results and Motivation
   - Collision-Dominated Incoherent Scatter
   - *D*-Region Experiments
   - Observational Results
3. Polar Mesosphere Summer Echoes (PMSE): Turbulent Source?
   - PMSE Review
   - PFISR Observations
   - Comparison to Theory

# Recent Advances in Incoherent Scatter Theory

Incoherent scatter theory in a nutshell - since the early 1960s

$$\langle |n_e(\mathbf{k},\omega)|^2 \rangle = \frac{|1+\chi_i|^2 \langle |n_e^0(\mathbf{k},\omega)|^2 \rangle + |\chi_e|^2 \langle |n_i^0(\mathbf{k},\omega)|^2 \rangle}{|1+\chi_e+\chi_i|^2}$$

- $n_\kappa^0(\mathbf{k},\omega)$ - Density fluctuation spectra for non-interacting particles
- $\chi_\kappa$ - Longitudinal susceptibility functions
- These functions involve complicated Gordeyev integrals, $J(\theta_\kappa)$, which depend on physics of plasma of interest
  $\rightarrow$ include formalisms for dealing with **B**, Coulomb collisions, and ion-neutral collisions - recent progress in all of these areas
- *Sulzer and González*, 1999; *Woodman*, 2004; *Kudeki and Milla*, 2006; *Milla and Kudeki*, 2006; *Rodrigues et al., 2007* (see also Kudeki CEDAR lecture, 2006) - recent progress in understanding collisional incoherent scatter spectral theory
  $\rightarrow$ Applicable especially to IS spectral and power measurements close to geomagnetic equator

# Measurements of the full ISR spectrum

Arecibo Observatory

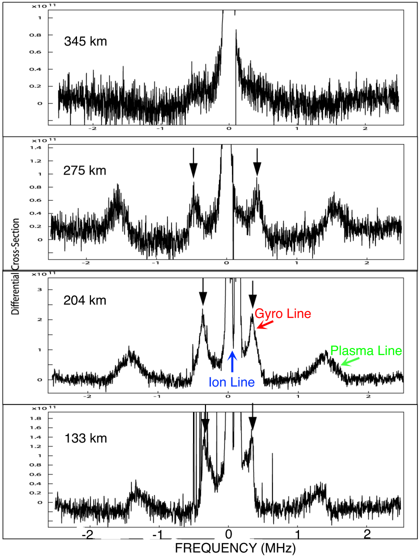


*Bhatt et al.*, *GRL*, 2006

## Ion Line

- Most IS measurements rely on central portion
- Sensitive to $N_e$, $T_e$, $T_i$, $V_{los}$, $\nu_{in}$, $\nu_{other}$, $N_i/N_e$

## Plasma Line

- Enhanced by photoelectrons to detectable levels in daytime
- Sensitive measure of $N_e$
- Used by most ISRs for calibration purposes, but numerous other applicationss

## Gyro Line

- "Theoretical" resonance discovered by *Salpeter* [1960]
- Only one unambiguous detection prior to this [*Behnke and Hagan*, 1978]
- High frequency end of whistler mode, approaches lower hybrid mode for oscillations $\perp$ **B**
- Probably numerous, unexploited applications

# Gyro Line as a Diagnostic

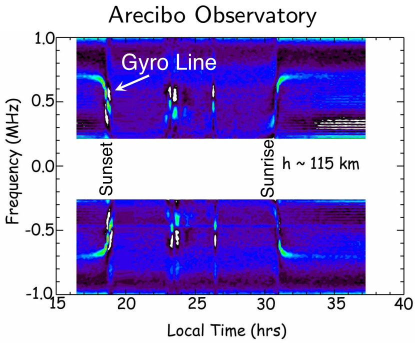


*Janches and Nicolls, GRL*, 2007

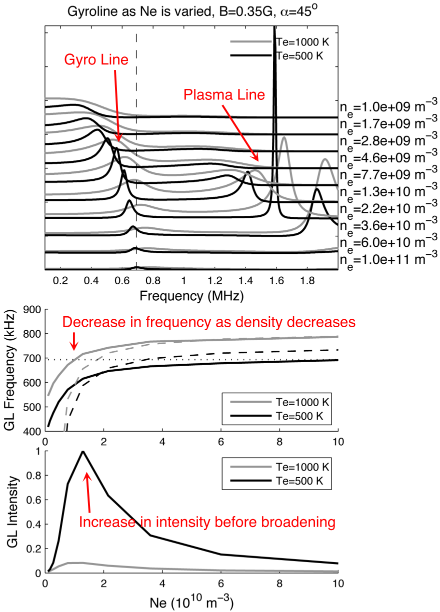


- High resolution measurements possible
- Well-predicted by theory
- Indicates potential to probe low-density sunset/sunrise *E* region

# Plasma Line “Splitting”

Plasma line appears to “split” or “jump” at first harmonic of the electron gyrofrequency

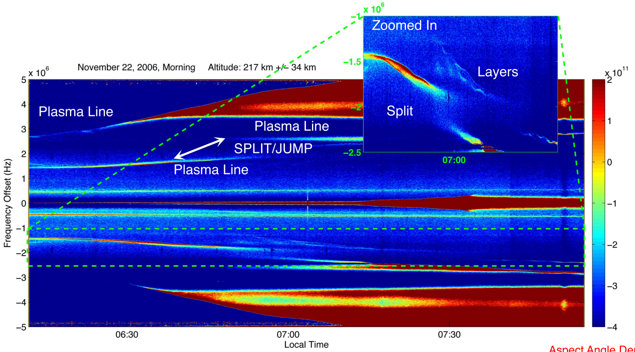


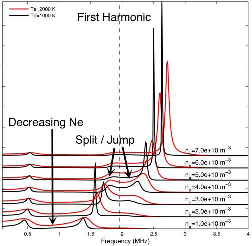


- Predicted by electron line theory (prior to measurements)
- Potential use as an ionospheric diagnostic
- Highly dependent on magnetic field aspect angle, as well as $T_e$

*Bhatt, Nicolls, et al., PRL*, 2008

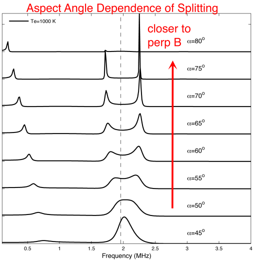

# High Resolution Plasma Line and Asymmetry

Using the asymmetry of the up- and down-shifted plasma lines, we can obtain an independent, high resolution measurement of $T_e$

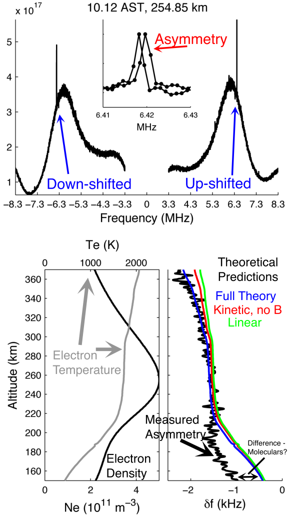


*Nicolls et al.*, *GRL*, 2006

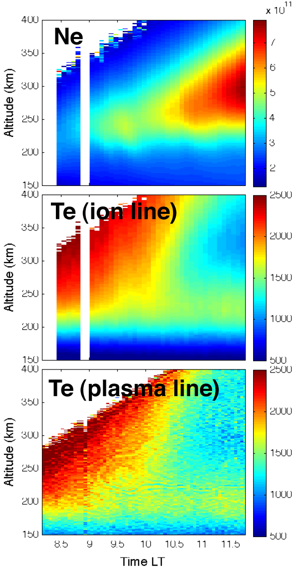

# Some Applications of HR Plasma Line and Asymmetry

Independent measures of $N_e$, $T_e$ allow for derivation of other unknowns, e.g., $M^+$ fractions

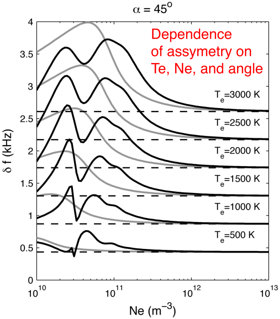


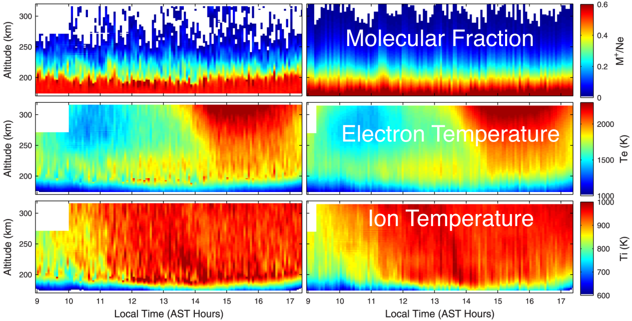


*Nicolls et al.*, *GRL*, 2006

*Aponte et al.*, *JGR*, 2007

Very applicable beyond Arecibo - nail down $T_i, T_e$ and $M^+$ in $F1$ region

# Some Applications of HR Plasma Line and Asymmetry

Independent measures of $N_e$, $T_e$ allow for derivation of other unknowns, e.g., $M^+$ fractions

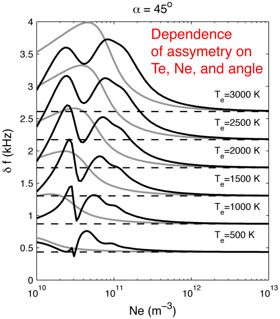


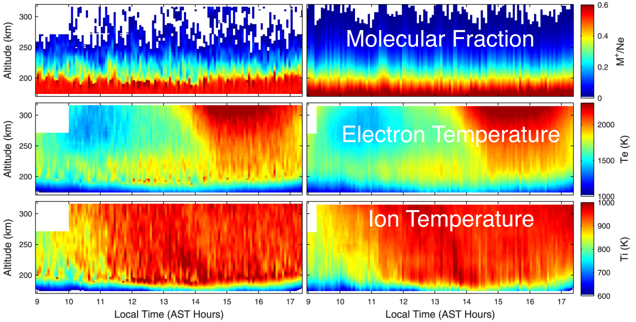


*Nicolls et al.*, *GRL*, 2006

*Aponte et al.*, *JGR*, 2007

Very applicable beyond Arecibo - nail down $T_i, T_e$ and $M^+$ in $F1$ region

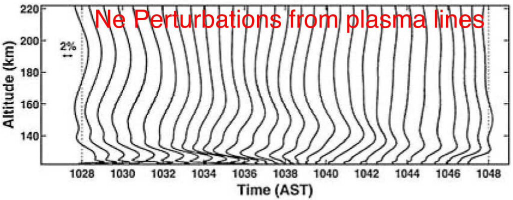


Gravity wave studies are another exciting new application of high resolution plasma line measurements (*Djuth et al.*, 1997,2004)

# Ion Gyroresonance Measurements at Jicamarca

*Rodrigues, Nicolls, et al. GRL*, 2007

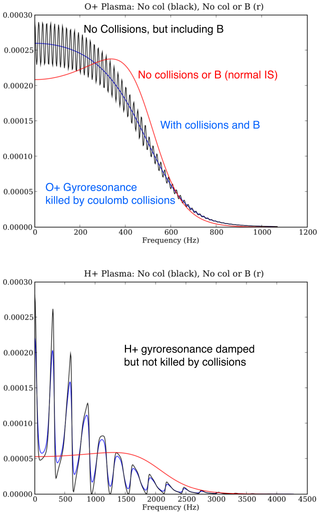


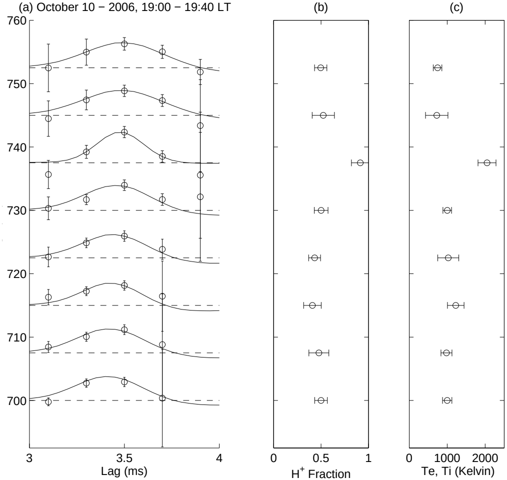


- Predicted $H^+$ gyroresonance for probing angles close to $\perp$ **B**
- First measurements since *Farley* [1967]
- Potential to supply additional information on $H^+$ fractions, $T_e$, $T_i$, $v_{H^+}$

# Outline

1. Incoherent Scatter - Recent Advances (My Bias)
   - Theoretical Advances
   - Experimental Advances
   - Observational Advances
2. Incoherent Scatter from the *D* Region: Observations with PFISR
   - Past Results and Motivation
   - Collision-Dominated Incoherent Scatter
   - *D*-Region Experiments
   - Observational Results
3. Polar Mesosphere Summer Echoes (PMSE): Turbulent Source?
   - PMSE Review
   - PFISR Observations
   - Comparison to Theory

# Motivation - Dynamics

- *D* region / MLT is an incredibly dynamical environment
- ISRs are one of the only systems for probing this region with the ability to resolve the dynamics

High Resolution Vertical Winds with Arecibo ISR

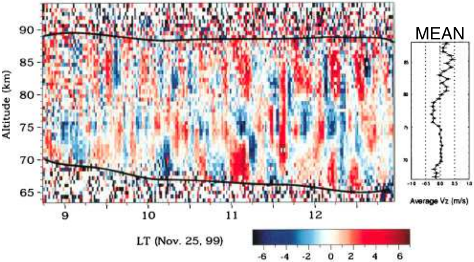


*Zhou*, *GRL*, 2000

- Arecibo measurements of vertical and horizontal winds and momentum fluxes

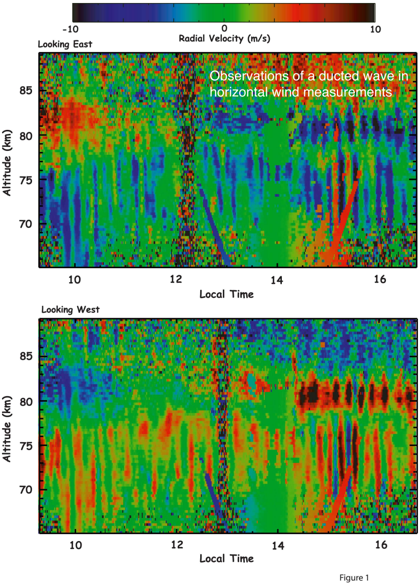


*Fritts and Janches*, *JGR*, 2008

# Motivation - Chemistry

Detection of meteoric smoke

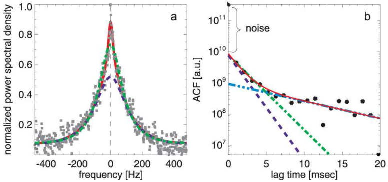


Spectra/ACF (above)

Derived MSP (below)

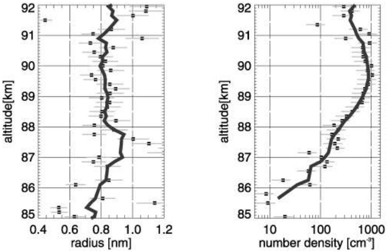


*Strelnikova et al.*, *GRL*, 2007

- Above 90 km $NO^+$, $O_2^+$ are the main constituents
- Positive ion clustering - e.g., $NO^+(N_2)$, $NO^+(CO_2)$
- Formation of hydrates - mainly $H^+(H_2O)_n$
- Formation of negative ions - e.g., $O_2^-$, $HCO_3^-$, $CO_3^-$
- Metallic species, meteoric smoke

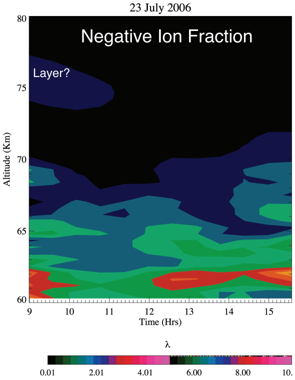


*Raizada et al.*, *JGR*, 2008

# Collision-Dominated Incoherent Scatter

- Plasma will be collisional if distance travelled between collisions $\ll \lambda_{\text{radar}}/4\pi$
- Ion random walk with characteristic correlation time $\sim$ time to travel $\lambda/4\pi$
- Different ways to deal with collisions in theory, all somewhat ad hoc

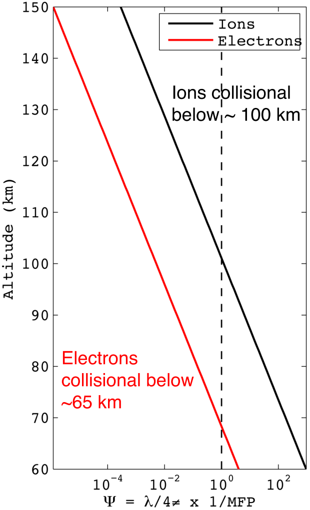


- "Electron line" is often not negligible in *D* region because of low $N_e$ (Debye length)

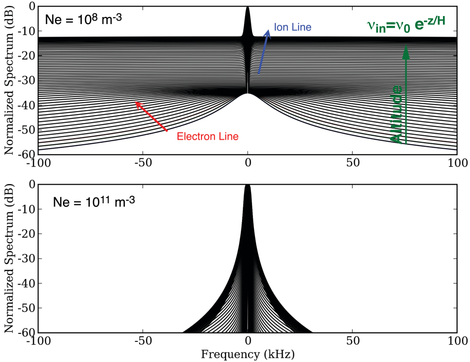


e.g., see *Mathews*, *JGR*, 1978

# $D$-Region Ionization

- Lyman-$\alpha$ - ionization of NO, daytime
- Solar x-rays and cosmic rays - ionization of all atmospheric constituents [<60 km]
- Primary auroral electrons - important above 60 km [10 keV electron beam produces ionization rate of $\sim 10^6\ \mathrm{m}^{-3}\mathrm{s}^{-1}$ at 70 km]
- Auroral bremsstrahlung x-rays can produce significant ionization from 50-70 km

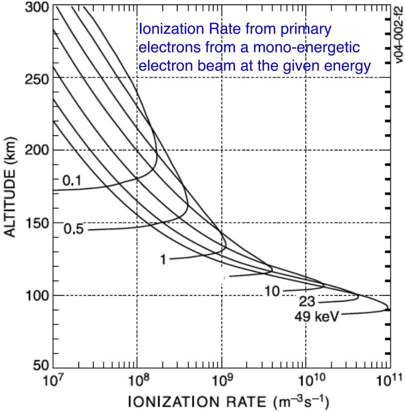


*Semeter and Kamalabadi*, *RS*, 2005

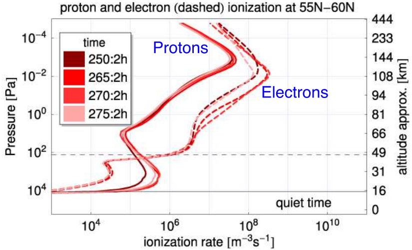


*Wissing and Kallerode*, *JGR*, 2009

$$q \approx \alpha n_e^2$$

$$\alpha \approx 2.5 \times 10^{-12} e^{-z/51.2}\ \mathrm{m}^3/\mathrm{s}$$

Ionization rate of $\sim 10^7\ \mathrm{m}^{-3}\mathrm{s}^{-1}$ at 80 km yields $N_e \sim 5 \times 10^9\ \mathrm{m}^{-3}$

# The Poker Flat ISR

- 128-panel AMISR system (upgraded from 96 in Sep. 07)
- Pulse-to-pulse steering capability
- ~1.6 MW peak Tx
- ~10% max duty cycle
- 4 reception channels
- Tx band 449-450 MHz
- 3.5 MHz max Rx bandwidth
- 4 $\mu$s min pulsewidth (freq. allocation limitation)
- Fully programmable, remotely operable/ted
- Graceful degradation - reliable operations


# Innovative Aspects and *D*-Region Measurables

- Spectral resolutions of $\sim$1 Hz
- Unambiguous, simultaneous zonal, meridional vertical winds at $\sim$few mins, $<$1 km res
- Observational capability during non-PCA conditions

$$S(f) \approx \frac{C}{\pi} \frac{\sigma}{(f - f_0)^2 + \sigma^2}$$

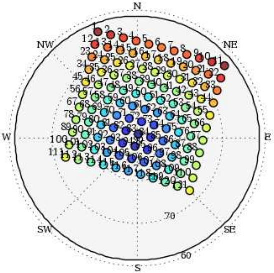


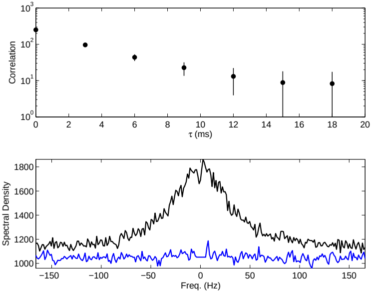


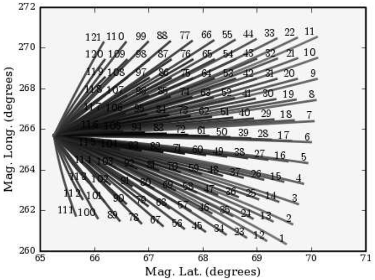

# Inertia-Gravity Wave Event - Densities

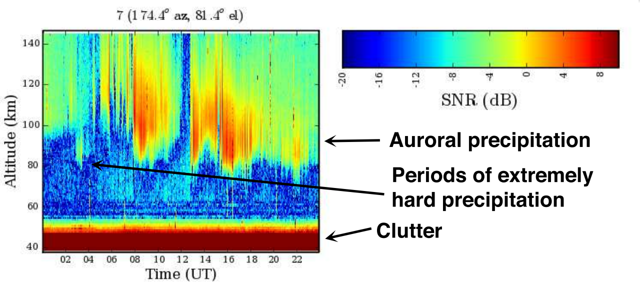


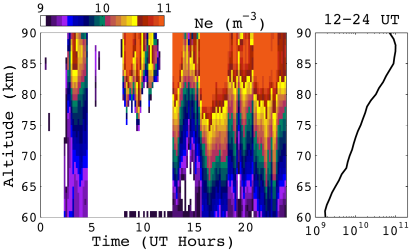


- Very intense electron precipitation throughout day on 04/23/2008
- Good SNR in *D*-region for 12+ hours, patchy signal early
- $N_e$ of $2 - 3 \times 10^9\ \mathrm{m}^{-3}$ at 60 km up to $\sim 10^{11}\ \mathrm{m}^{-3}$ at 95 km

See also *Janches et al.*, *JASTP*, 2009

# Inertia-Gravity Wave Event - Spectra

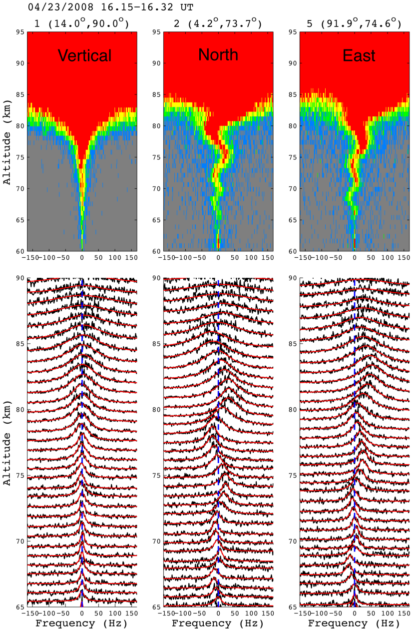


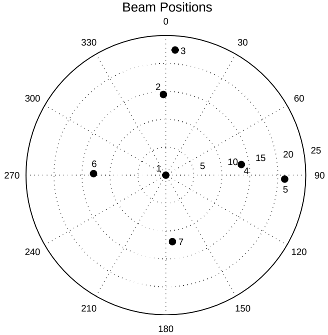


- 7-beam experiment, field-of-view <20-30 km
- Representative 10-minute spectra from 3 beams (up, north, east) show extremely precise measurements with clear wave activity
- Lorentzian fits to spectra give LOS speeds with errors <0.1-0.2 m/s below 75 km and widths with errors <1-2 Hz

# Inertia-Gravity Wave Event - Resolved Winds

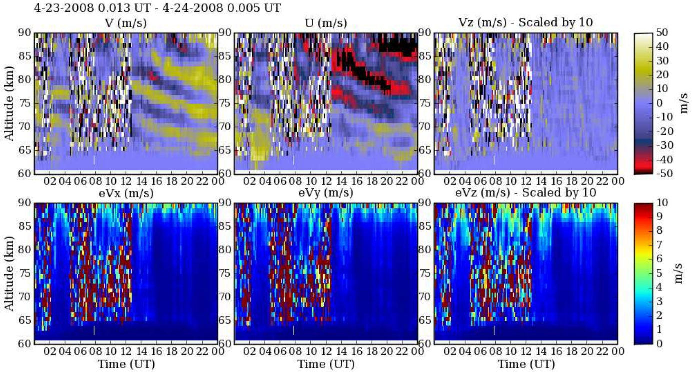


- Radial speeds are resolved into extremely robust winds
- Correlation analysis indicates stationary wave field (large horizontal wavelength)
- Vertical speeds extremely small
- Periods of sufficient ionization are marked by clear long-period (10+ hr) wave activity, 5-10 km vertical wavelength
- Wind amplitudes of $\pm 50\ \mathrm{m/s}$
- $90^\circ$ phase difference between $U$ and $V$
- Anticyclonic (clockwise) rotation with altitude

# Spectral Width Information

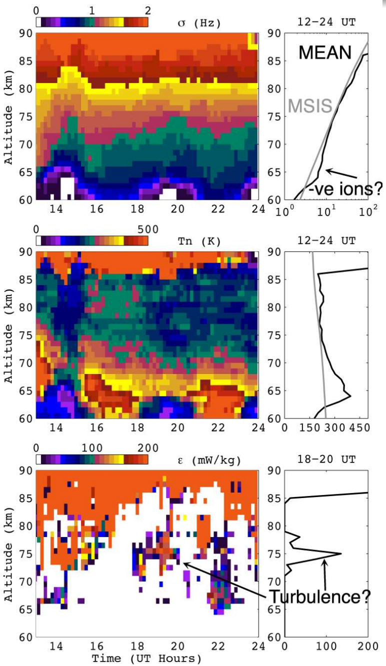


$$\sigma \approx \frac{16\pi k_B T}{\lambda_R^2 m_i \nu_{in}}(1+\lambda)$$

- (Top) Log10 of spectral width; average (black), MSIS (gray)
  - Above 75 km, same scale height as MSIS; below 75 km, spectral "hump" indicates presence of negative ions - $\lambda \sim 1$
- (Middle) Derived $T_n$ assuming MSIS $\nu_{in}$
  - 75-85 km, excellent agreement with MSIS
- (Bottom) Derived turbulence energy dissipation rate, $\epsilon$, from velocity variance of scatterers
  - $\epsilon$ increases from 70-80 km, between 18-20 UT

# Background Winds and Wave Amplitude

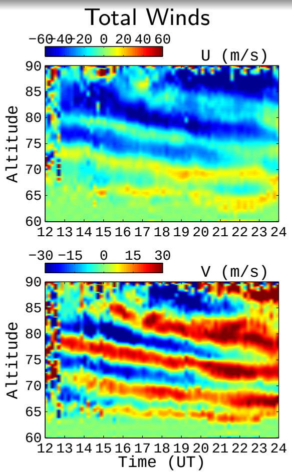


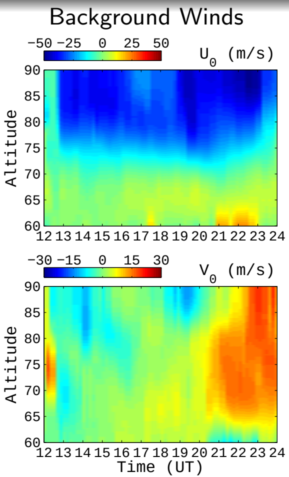


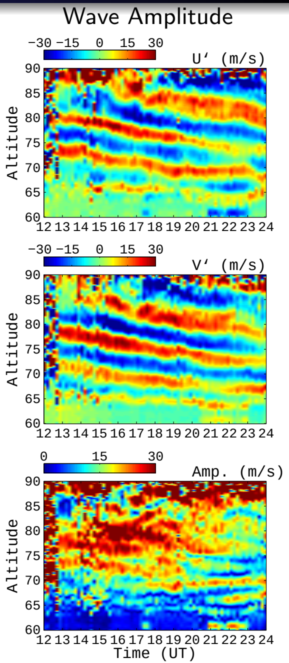


- Background wind dominated by westward wind above 75 km
- Winds accelerate by ~15 m/s northward after 20 UT
- Wave amplitudes increasing with altitude, $\sim \pm 30$ m/s
- Wave amplitude decreases by $\sim 15$ m/s after 20 UT

# Direction of Propagation

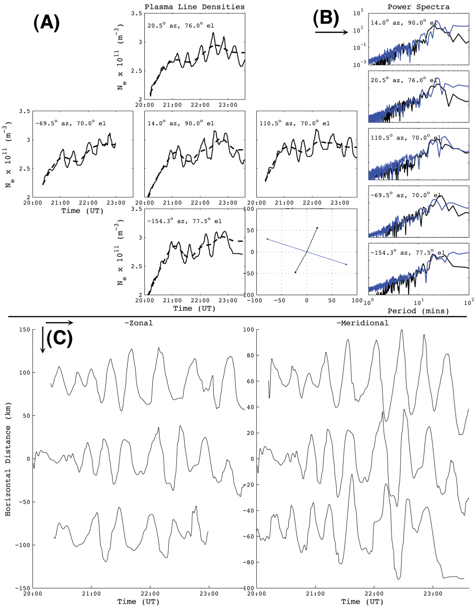


- Often able to directly determine propagation direction from beam-to-beam cross-correlations (e.g., *Vadas and Nicolls, JASTP*, 2009)
- Some waves, however, have $\lambda_H \gg$FOV - not possible to determine $\lambda_H$ directly

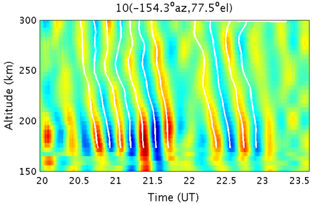


*Vadas and Nicolls, JASTP*, 2009

# Direction of Propagation

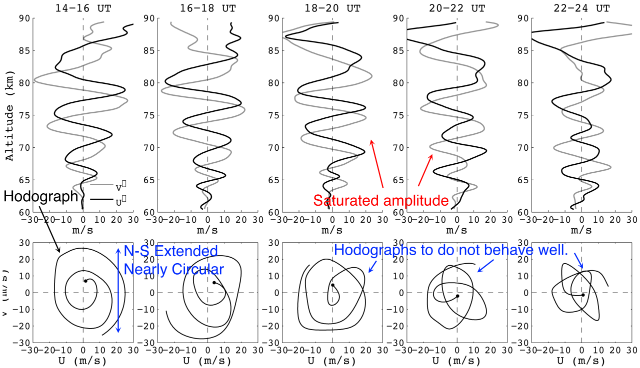


$$u' = \left(\frac{i\omega_{Ir} k - f\ell}{i\omega_{Ir}\ell + fk}\right) v'$$

$$\tilde{\sigma} = \frac{\delta\sigma}{\bar{\sigma}} = \tilde{T} - \tilde{\rho} = 2\tilde{T} - \frac{\tilde{p}}{R\bar{T}}$$

$$= \frac{2m}{g}\frac{\omega_{Ir}^2 - f^2}{\omega_{Ir}^2 k^2 + f^2\ell^2}(i\omega_{Ir} k + f\ell)\tilde{u}$$

- Hodograph analysis in altitude and time gives direction of propagation and ground-relative period (as a function of altitude)
- Spectral width and $w'$ phase relation also contains information
- This wave most likely propagating mainly northward ($\pm 10°$), close to inertial period

# Evidence for Saturation, Dynamic Instability

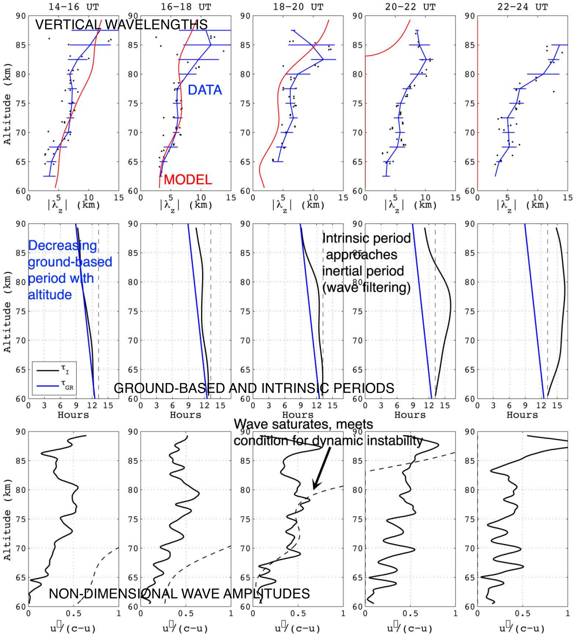


$$m^2 \approx \frac{k_H^2(N^2 - \omega_{Ir}^2)}{\omega_{Ir}^2 - f^2}$$

$$\omega_{Ir} = \omega - k_H U_H \quad (\text{IntrinsicFrequency})$$

$$\lambda_H \sim 1500 - 2000 \text{ km}$$

- Vertical wavelength increasing with altitude
- Ground-relative frequency increases with altitude (nature of source)
- Intrinsic frequency approaches inertial frequency as winds accelerate

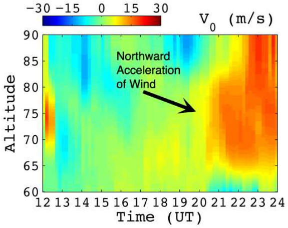


- Non-dimensional amplitude approaches dynamical instability criterion (*Fritts and Rastogi*, *RS*, 1985)
- Wave amplitude decreases → winds accelerate → suicidal wave!

# Inertial Gravity Wave Event - Source?

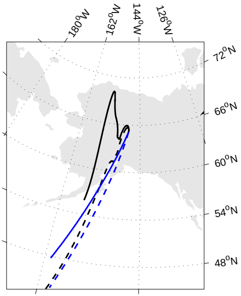


HWM07 (Black), No Winds (Blue)

- Reverse ray tracing can yield source information
- Extremely sensitive to winds (e.g., HWM07, black) and initial wave conditions
- This wave likely took several days to reach 60 km altitude
- Potential source 5 days earlier - significant geostrophic adjustment to the south of Alaska, should radiate large-period IGWs

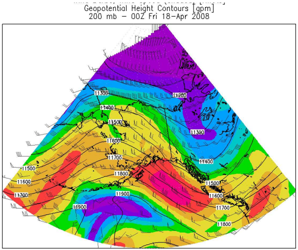


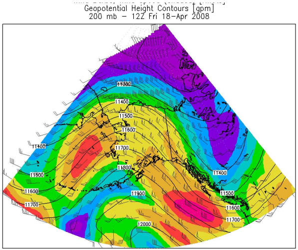


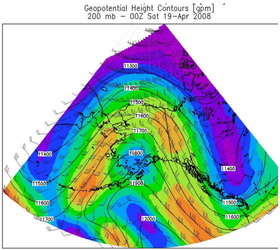

# Outline

# PMSE: What Are They?

- Peculiar irregularities discovered in the late 1970s, strongest in vertical direction
- Enhanced returns in cold summer mesopause region
- Associated with ice particles and neutral turbulence
- Strongly frequency-dependent in occurrence statistics and reflectivity

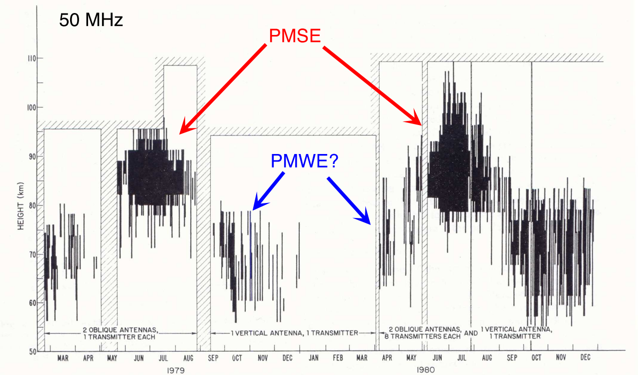


Fig. 1. Height of occurrence of mesospheric echoes on a daily basis from February 1979 to December 1980.

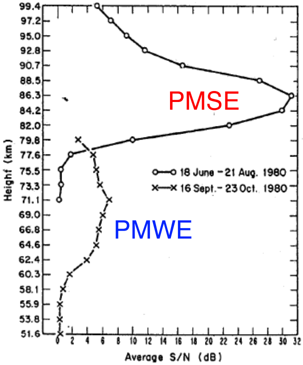


*Ecklund and Balsley, JGR*, 1981

# Link to ice and NLCs/PMCs, Basic Phenomenology

- Ice particle nucleation on existing ice nuclei (e.g., meteoric smoke)
- Sedimentation and growth 87-89 km (mesopause), transport (winds, waves, turbulence)
- $\sim$85 km ($\sim$30 nm), ice particles are large enough to be seen optically
- Particles are immersed in $D$ region - electron attachment
- Turbulence leads to electron density fluctuations

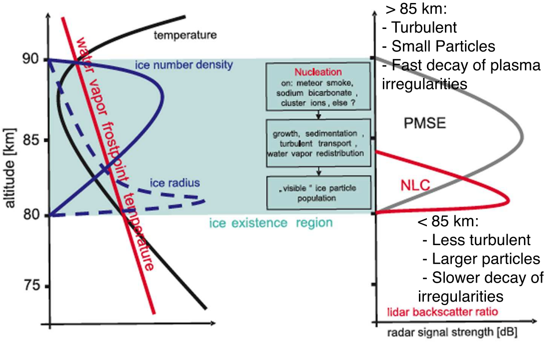


*Rapp and Thomas, JASTP*, 2006

Hence, strong, general correlation between NLC and PMSE

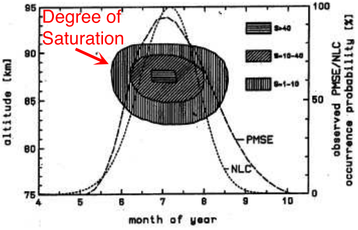


*Lubken, JGR*, 1999

# $N_e$ Biteouts / Negatively Charged Particles

Electron density biteouts within PMSE

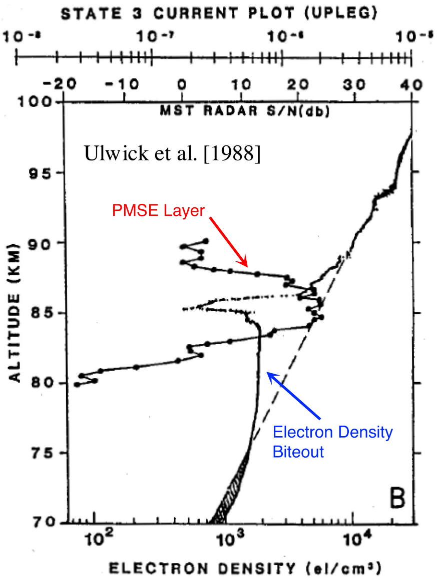


Evidence for negatively charged particles

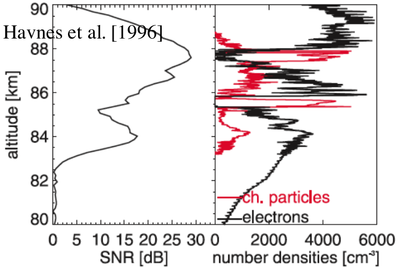


But don't always carry that much charge

...Important..

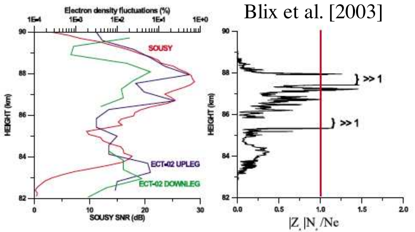

# Turbulence as the Source of PMSE

- Extremely high turbulent energy dissipation rate would be required to explain observations at sub-meter wavelengths
- Max value implies that only HF radars could see PMSE

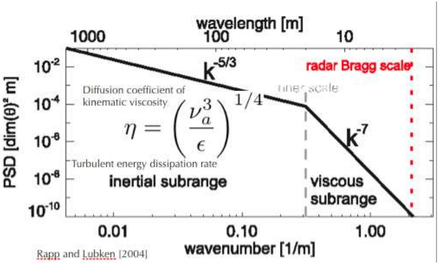


Kolmogorov microscale, $\eta$ - where turbulent and molecular diffusion are equal

# Turbulence as the Source of PMSE

- Extremely high turbulent energy dissipation rate would be required to explain observations at sub-meter wavelengths
- Max value implies that only HF radars could see PMSE

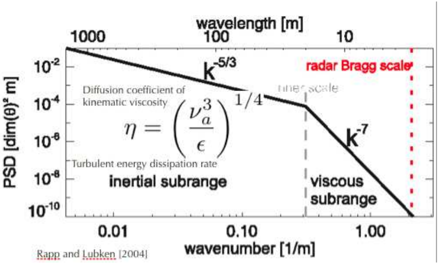


Kolmogorov microscale, $\eta$ - where turbulent and molecular diffusion are equal

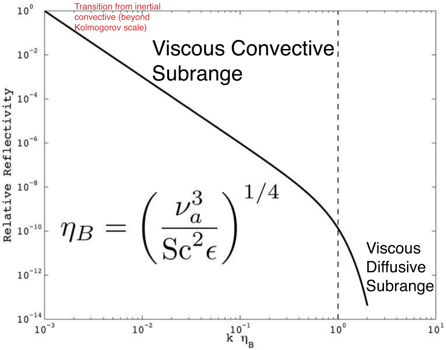


- Electron irregularity dissipation rate can be slower than dissipation of energy (Kolmogorov), because of the braking effects of massive (multiply?) charged ions (ice particles)
- Ratio of the diffusion rates is $\mathrm{Sc} = \nu_a / D_e$ (diffusion coefficient of kinematic viscosity to particle diffusion rate of electrons)
- Dissipation is Batchelor - particle density squared rather than energy (velocity squared)
- First proposed as the explanation for PMSE by *Kelley et al.*, 1987; *Cho et al.*, 1992

# Neutral Turbulence and PMSE

*Cho et al.* [1992] theory did not agree with measurements in two significant ways:

1. Evidence for direct link to neutral turbulence is dubious (right)
2. Theory predicted that $|Z|N_A/N_e > 1 - 1.2$ for diffusion to be slowed (below)

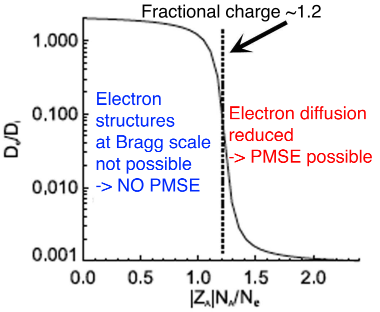


Adapted from *Cho et al.* [1992] by *Rapp and Lubken* [2004].

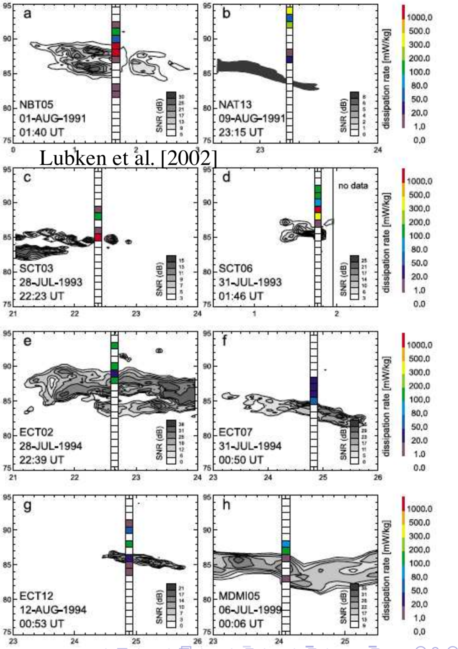

# Diffusion in the Vicinity of Charged Ice

- Multi-component plasma (electrons, positive ions, aerosol particles)
- Each satistifies a continuity equation $\frac{\partial N_j}{\partial t} + \nabla \cdot \Gamma_j = 0$
- Two diffusion modes - one ($D_1$) due to electrons + positive ions, the other ($D_2$) due to electrons + charged aerosols
- $\Lambda = |Z_A| N_A / N_e$ is the abundance ratio and is critically important
- $D_1$ - fast diffusion mode, varies strongly with $\Lambda$ but independent of aerosol properties
- $D_2$ - slow diffusion mode ($\sim D_A$ for $\Lambda$ small): Large Schmidt numbers are associated with long diffusion times - Fossils
- Real case is some combination - Simulations (*Rapp and Lubken*, 2003) show decay at $D_1$ to amplitude of around $\sim$0.5

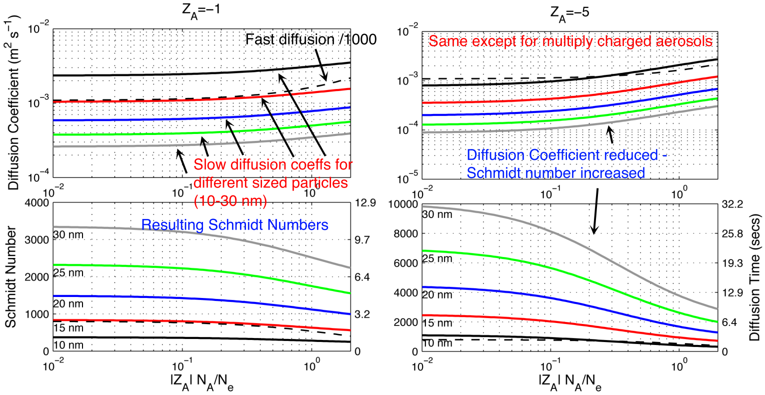


*Nicolls et al., JASTP*, 2009 - see also *La Hoz et al., JGR*, 2006

# PMSE Layer "Imaging" with PFISR

Patches of PMSE during daytime conditions over entire FOV (∼65 km at 85 km altitude)

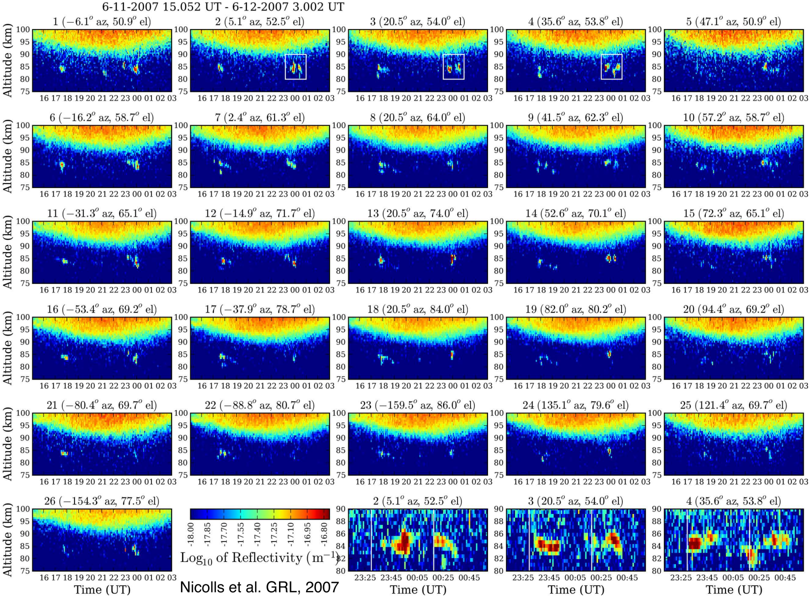


Nicolls et al. GRL, 2007

# PMSE Layer “Imaging” with PFISR

Coherent PMSE patches “drift” in - strongly implies fossilization of structures

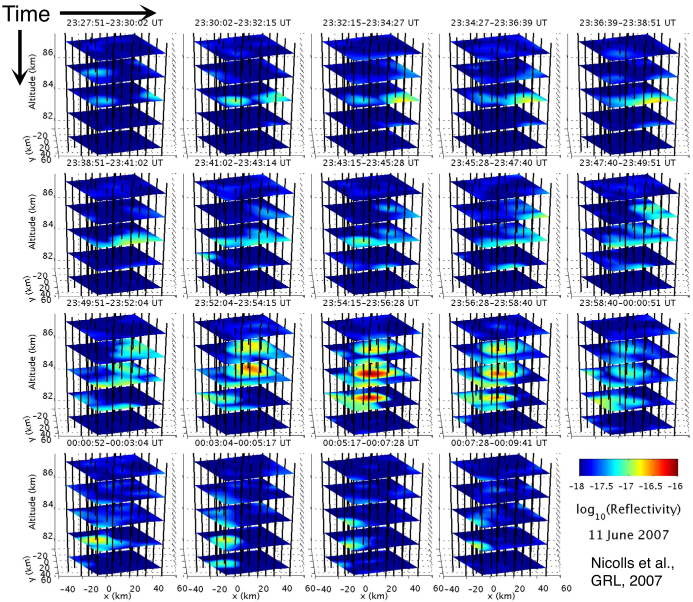


11 June 2007

Nicolls et al., GRL, 2007

# NLC-PMSE Comparions

Similar structure/motions in PMSE/NLC observations - further evidence for fossilization

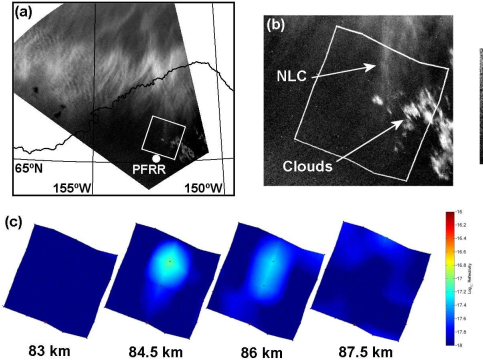


Enhanced PMSE at times of small-scale billows / structures in NLCs

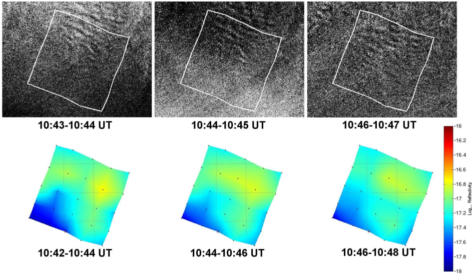


- First common volume comparisons of spatially resolved PMSE, NLC, and PMC structures

*Taylor et al., JASTP*, 2009

PMSE layer above Lidar NLC layer
- Smaller particles in PMSE

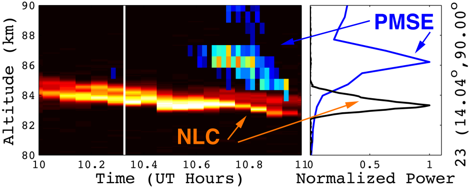

# Why a higher frequency ISR is useful

1. Beam/Shear broadening effects reduced
2. Measurement of background parameters
3. Scatter may better represent index of refraction variations due to energy dissipation
4. Aspect-insensitive scatter suggests well into the dissipation range
5. Pushing boundary of turbulence theories

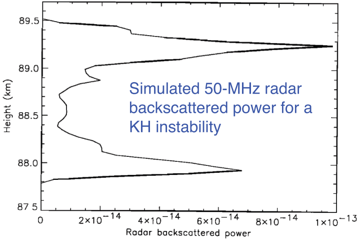


*Gibson-Wilde et al.*, *RS*, 2000

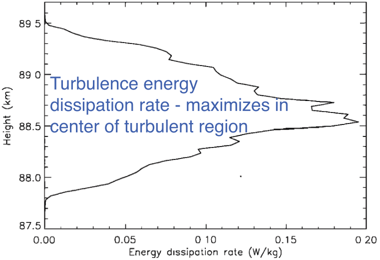


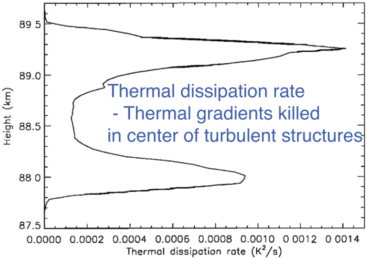

# Turbulence from ISRs

Vertical wavenumber spectrum
(*Fritts and van Zandt, JAS*, 1993)

$E_0 = \frac{N^2}{10m_*^2}$ - Kinetic energy

Energy dissipation rate:

$$\epsilon \approx \frac{NE_0}{18m_*}\left(\frac{1}{H} - \frac{3}{2H_E}\right)$$

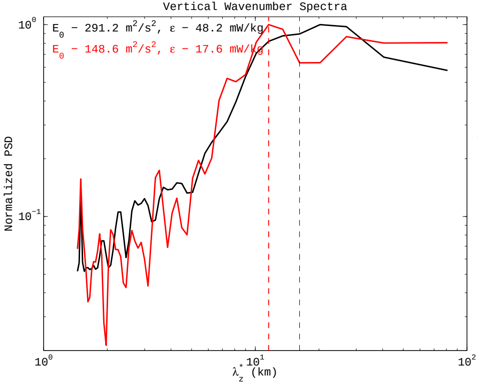


Vertical velocity variance
(directly or from spectral width
measurements)

$$\epsilon \approx C\sigma_V^2 N$$

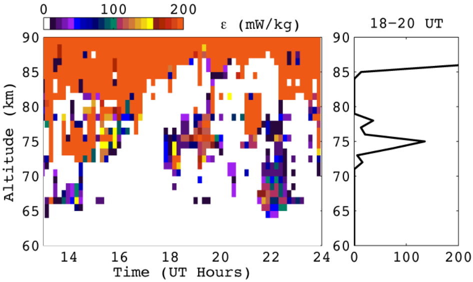


Potential for high resolution turbulence
studies with these methods.
e.g., see *Hocking, RS*, 1985

# PFISR Observations - Absolute Reflectivity

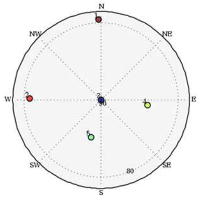


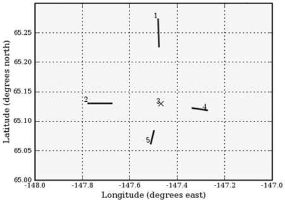


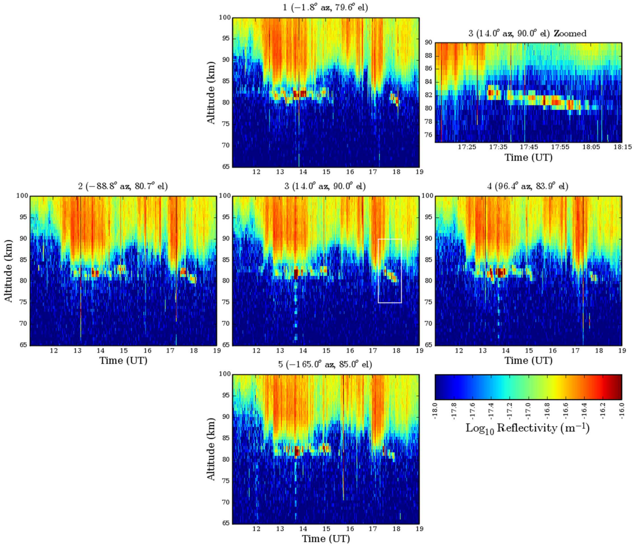


- Absolute reflectivity in line with expectations
- Aspect insensitive (down to at least $\sim 55^\circ$)

*Nicolls et al.*, *JASTP*, 2009

# Spectral Observations - Vertical Beam

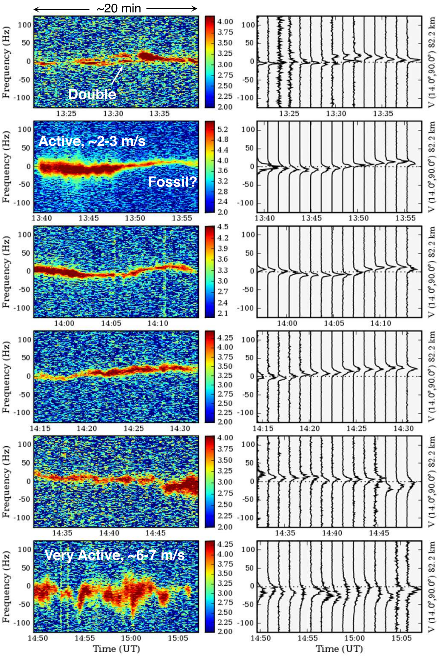


- 5-second, single altitude spectra from vertical beam
- 5 consecutive 20-minute windows
- $\pm\sim$10 m/s vertical velocities
- Transition from extremely narrow spectra (well-behaved) to extremely broad spectra (more dynamic)
- Perhaps several regions of active turbulence
- Split echoes - evidence for unresolved features

  *Nicolls et al.*, *JASTP*, 2008

# Spectral Observations - All Beams

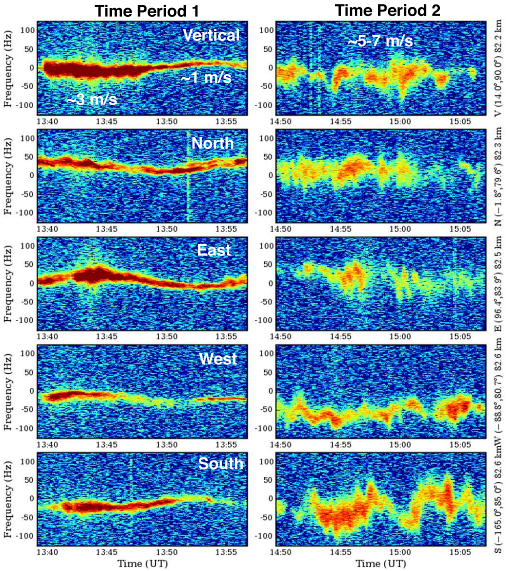


- Echoes from all beams during two 20-minute windows
- Spectra during “non-turbulent” and “turbulent” time periods show dramatically different characteristics
- Non-turbulent echoes show consistency from beam-to-beam and with motion with a background wind field; turbulent echoes do not
- Non-turbulent echoes show a period of enhanced power and spectral width which decays into narrow returns - fossilization of echoes?
- Non turbulent echoes - spectral widths of ∼3 m/s (∼ 100 mW/kg) , decay to widths of ∼1-2 m/s (∼ 10 W/kg)
- Turbulent echoes - spectral widths of ∼5-7 m/s (∼ 500 mW/kg)

*Nicolls et al., JASTP*, 2009

# Schmidt Numbers

Schmidt number as a function of spectral width, assuming Batchelor shape, $\eta_B = \left(\frac{\nu_a^3}{\mathrm{Sc}^2\epsilon}\right)^{1/4}$

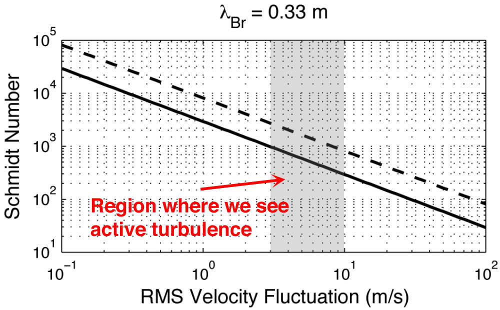


*Nicolls et al., JASTP*, 2009

- Spectral widths of ∼1-2 m/s imply Schmidt numbers of 3000-8000 **(but, it is unlikely that this is active turbulence)**
- Spectral widths of 5-7 m/s imply Schmidt numbers of 500-1200
- Are these numbers reasonable for particle sizes and charge numbers in the mesopause?

# Diffusion in the Vicinity of Charged Ice

## Conclusions from the diffusion analysis

- Schmidt numbers of several thousand can be obtained for all values of Λ
- PMSE at higher frequencies is likely associated with large particles $> 20 - 30$ nm ($D_2$ goes as particle radius squared)
- Large Schmidt numbers are associated with long diffusion times
- If narrow echoes are associated with weak turbulence, but exist in the presence of strongly enhanced Schmidt numbers, they will persist for longer times - explains their predominance

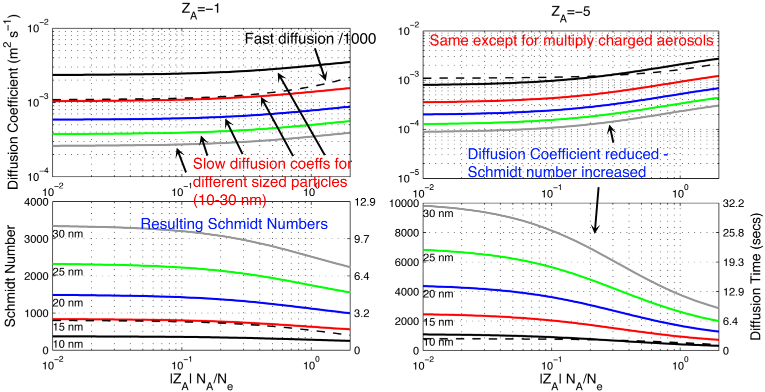


*Nicolls et al., JASTP*, 2009 - see also *La Hoz et al., JGR*, 2006

# Gravity Wave and Vertical Velocity

- Clear evidence of a ∼20-minute wave
- Spectral widths larger during upward phase of wave - larger turbulence dissipation rate
- GWs are more convectively/dynamically unstable during their upward phase
- Enhanced turbulent region logically due to breaking of wave
- Diffusion time of ∼30 seconds is consistent with observations

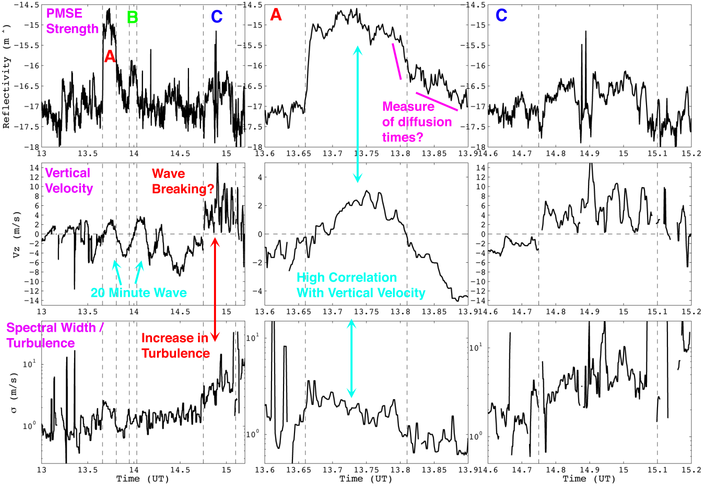

# Summary

1. Incoherent Scatter theory and observations are still evolving.
   - Understanding of IS theory in different regimes still being investigated.
   - Observational capabilities are always being improved.
   - Improved coding and analysis techniques are solving major observational limitations.

# Summary

1. Incoherent Scatter theory and observations are still evolving.
   - Understanding of IS theory in different regimes still being investigated.
   - Observational capabilities are always being improved.
   - Improved coding and analysis techniques are solving major observational limitations.
2. Studies of the $D$ region and MLT is unchartered territory for ISRs
   - Ability to extract wind and waves with high temporal and altitudinal resolution, much like lidars.
   - Ability to identify lower atmospheric sources and propagation paths - understanding the sources and effects of atmospheric waves observed in the mesosphere and thermosphere is now of major scientific importance.
   - Ability to identify turbulent regions, momentum fluxes, wave saturation.

# Summary

1. Incoherent Scatter theory and observations are still evolving.
   - Understanding of IS theory in different regimes still being investigated.
   - Observational capabilities are always being improved.
   - Improved coding and analysis techniques are solving major observational limitations.
2. Studies of the *D* region and MLT is unchartered territory for ISRs
   - Ability to extract wind and waves with high temporal and altitudinal resolution, much like lidars.
   - Ability to identify lower atmospheric sources and propagation paths - understanding the sources and effects of atmospheric waves observed in the mesosphere and thermosphere is now of major scientific importance.
   - Ability to identify turbulent regions, momentum fluxes, wave saturation.
3. Measurements with ISRs are showing that causal mechanisms for PMSE are understood.
   - Allows for interpretation of PMSE in terms of turbulence theories.
   - Can use PMSE to study the microphysics and charging of mesospheric ice particles.
   - Investigations of variability, plasma instabilities, electric field structures
   - Spatially resolved, coordinated measurements will help us understand anthropogenic influences on the mesospheric environment.

# Section 1 References (Incoherent Scatter)


- Aponte N., M. P. Sulzer, M. J. Nicolls, R. Nikoukar, and S. A. Gonzalez, Molecular ion composition measurements in the F1 region at Arecibo, J. Geophys. Res., 112, A06322, doi:10.1029/2006JA012028, 2007.
- Bhatt A. N., E. A. Gerken Kendall, M. C. Kelley, M. P. Sulzer, E. B. Shume, Observations of strong gyro line spectra at Arecibo near dawn, Geophys. Res. Lett., 33, L14105, doi:10.1029/2006GL026139, 2006.
- Bhatt A. N., M. J. Nicolls, M. P. Sulzer, and M. C. Kelley, Observations of plasma line splitting in the ionospheric incoherent scatter spectrum, Phys. Rev. Lett., 100(4), doi:10.1103/PhysRevLett.100.045005, 2008.
- Djuth, F. T., M. P. Sulzer, J. H. Elder, and V. B. Wickwar, High-resolution studies of atmosphere-ionosphere coupling at Arecibo Observatory, Puerto Rico, Radio Sci., 32(6), 23212344, 1997.
- Djuth, F. T., M. P. Sulzer, S. A. Gonzáles, J. D. Mathews, J. H. Elder, and R. L. Walterscheid, A continuum of gravity waves in the Arecibo thermosphere?, Geophys. Res. Lett., 31, L16801, doi:10.1029/2003GL019376, 2004.
- Farley, D. T., Proton Gyroresonance Observed in Incoherent Scattering from the Ionosphere, Phys. Fluids, 10, 1584, 1967.
- Janches D. J. and M. J. Nicolls, Diurnal variability of the gyro resonance line observed with the Arecibo incoherent scatter radar at E- and F1-region altitudes, Geophys. Res. Lett., 34, L01103, doi:10.1029/2006GL028510, 2007.
- Kudeki, E., and M. Milla, Incoherent scatter spectrum theory for modes propagating perpendicular to the geomagnetic field, J. Geophys. Res., 111, A06306, doi:10.1029/2005JA011546, 2006.
- Milla, M. and E. Kudeki, F-region electron density and Te / Ti measurements using incoherent scatter power data collected at ALTAIR, Ann. Geophys., 24, 5, 1333-1342, 2006.
- Nicolls M. J., M. P. Sulzer, N. Aponte, R. Seal, R. Nikoukar, and S. A. Gonzalez, High resolution electron temperature measurements using the plasma line asymmetry, Geophys. Res. Lett., 33, L18107, doi:10.1029/2006GL027222, 2006.
- Rodrigues F. S, M. J. Nicolls, and D. L. Hysell, Improved electron density measurements at Jicamarca, J. Geophys. Res., 112, A11315, doi:10.1029/2007JA012598, 2007.
- Rodrigues F. S., M. J. Nicolls, R. Woodman, D. L. Hysell, J. L. Chau, and S. A. Gonzalez, Ion gyroresonance observations at Jicamarca revisited, Geophys. Res. Lett., 34, L13107, doi:10.1029/2007GL029680, 2007.
- Sulzer, M. P., and S. Gonzalez, The effect of electron Coulomb collisions on the incoherent scatter spectrum in the F region at Jicamarca, J. Geophys. Res., 104(A10), 22,53522,551, 1999.
- Woodman, R. F., On a proper electron collision frequency for a Fokker-Planck collision model with Jicamarca applications, J. Atmos. Solar-Terr. Phys., 66, 17, 1521-1541, 2004.

# Section 2 References ($D$ Region)


- Fritts, D. C., and D. Janches, Dual-beam measurements of gravity waves over Arecibo: Reevaluation of wave structure, dynamics, and momentum fluxes, J. Geophys. Res., 113, D05112, doi:10.1029/2007JD008896, 2008.
- Fritts, D. C., and P. K. Rastogi, Convective and dynamical instabilities due to gravity wave motions in the lower and middle atmosphere: Theory and observations, Radio Sci., 20(6), 12471277, 1985.
- Fritts and Yuan, Stability Analysis of Inertio-Gravity Wave Structure in the Middle Atmosphere, J. Atmos. Sci., 46, 12, 1738-1745, 1989.
- Heinselman C. J. and M. J. Nicolls, A Bayesian approach to electric field and E -region neutral wind estimation with the Poker Flat Advanced Modular Incoherent Scatter Radar, Radio Sci., 43, RS5013, doi:10.1029/2007RS003805, 2008.
- Hocking W. K., Measurement of turbulent energy dissipation rates in the middle atmosphere by radar techniques: A review, Radio Sci., 20, 6, 1403-1422, 1985.
- Janches, D., D. C. Fritts, M. J. Nicolls and C. J. Heinselman, Observations of D-region Structure and Atmospheric Tides with PFISR during Active Aurora, J. Atmos. Solar-Terr. Phys., 71, 688-696, 2009.
- Mathews, J., The Effect of Negative Ions on Collision-Dominated Thomson Scattering, J. Geophys. Res., 83(A2), 505-512, 1978.
- Nicolls M. J., C. J. Heinselman, Three-dimensional measurements of traveling ionospheric disturbances with the Poker Flat Incoherent Scatter Radar, Geophys. Res. Lett., 34, L21104, doi:10.1029/2007GL031506, 2007.
- Nicolls M. J., et al., Case Study of an Inertia Gravity Wave in the Mesosphere over Alaska with the Poker Flat Incoherent Scatter Radar, J. Geophys. Res., To be submitted, 2009.
- Raizada S., M. P. Sulzer, C. A. Tepley, S. A. Gonzalez, M. J. Nicolls, Inferring D region parameters using improved incoherent scatter radar techniques at Arecibo, J. Geophys. Res., 113, A12302, doi:10.1029/2007JA012882, 2008.
- Semeter J., F. Kamalabadi, Determination of primary electron spectra from incoherent scatter radar measurements of the auroral E region, Radio Sci., 40, RS2006, doi:10.1029/2004RS003042, 2005.
- Strelnikova I., M. Rapp, S. Raizada, M. Sulzer, Meteor smoke particle properties derived from Arecibo incoherent scatter radar observations, Geophys. Res. Lett., 34, L15815, doi:10.1029/2007GL030635, 2007.
- Vadas S. L., M. J. Nicolls, Using PFISR measurements and gravity wave dissipative theory to determine the neutral, background thermospheric winds, Geophys. Res. Lett., 35, L02105, doi:10.1029/2007GL031522, 2008.
- Vadas S. L. and M. J. Nicolls, Temporal Evolution of Neutral, Thermospheric Winds and Plasma Response using PFISR Measurements of Gravity Waves, J. Atmos. Solar-Terr. Phys, 71, 740-770, 2009.
- Wissing J. M., M.-B. Kallenrode, Atmospheric Ionization Module Osnabrck (AIMOS): A 3-D model to determine atmospheric ionization by energetic charged particles from different populations, J. Geophys. Res., 114, A06104, doi:10.1029/2008JA013884, 2009.
- Zhou, Q., Incoherent Scatter Radar Measurement of Vertical Winds in the Mesosphere, Geophys. Res. Lett., 27(12), 1803-1806, 2000.

# Section 3 References (PMSE)


- Blix T. A., M. Rapp, and F. J. Lubken, Relations between small scale electron number density fluctuations, radar backscatter, and charged aerosol particles, J. Geophys. Res., 108 (D8), 8450, doi:10.1029/2002JD002430, 2003.
- Cho, J., T. Hall, and M. Kelley, On the Role of Charged Aerosols in Polar Mesosphere Summer Echoes, J. Geophys. Res., 97(D1), 875-886, 1992.
- Ecklund, W., and B. Balsley, Long-Term Observations of the Arctic Mesosphere with the MST Radar at Poker Flat, Alaska, J. Geophys. Res., 86(A9), 7775-7780, 1981.
- Fritts D. C. and T. E. VanZandt, Spectral estimates of gravity wave energy and momentum fluxes. Part I: energy dissipation, acceleration and constraints, J. Atmos. Sci., 50, 3685-3694, 1993.
- Gibson-Wilde, D., J. Werne, D. Fritts, and R. Hill, Direct numerical simulation of VHF radar measurements of turbulence in the mesosphere, Radio Sci., 35(3), 783-798, 2000.
- Havnes, O., J. Troim, T. Blix, W. Mortensen, L. Nsheim, E. Thrane, and T. Tnnesen, First detection of charged dust particles in the Earth's mesosphere, J. Geophys. Res., 101(A5), 10839-10847, 1996.
- La Hoz C., O. Havnes, L. I. Naesheim, D. L. Hysell, Observations and theories of Polar Mesospheric Summer Echoes at a Bragg wavelength of 16 cm, J. Geophys. Res., 111, D04203, doi:10.1029/2005JD006044, 2006.
- Lubken, F.-J. Thermal structure of the Arctic summer mesosphere. J. Geophys. Res. 104 (D8), 91359149, 1999.
- Lubken, F.-J., M. Rapp, and P. Hoffmann, Neutral air turbulence and temperatures in the vicinity of polar mesosphere summer echoes, J. Geophys. Res., 107(D15), 4273, doi:10.1029/2001JD000915, 2002.
- Kelley, M., D. Farley, and J. Rottger, The Effect of Cluster Ions on Anomalous VHF Backscatter from the Summer Polar Mesosphere, Geophys. Res. Lett., 14(10), 1031-1034, 1987.
- Nicolls M. J., C. J. Heinselman, E. A. Hope, S. Ranjan, M. C. Kelley, J. D. Kelly, Imaging of Polar Mesosphere Summer Echoes with the 450 MHz Poker Flat Advanced Modular Incoherent Scatter Radar, Geophys. Res. Lett., 34, L20102, doi:10.1029/2007GL031476, 2007.
- Nicolls, M. J., M. C. Kelley, R. H. Varney, C. J. Heinselman, Spectral observations of polar mesospheric summer echoes at 33 cm (450 MHz) with the Poker Flat Incoherent Scatter Radar, J. Atmos. Solar-Terr. Phys., 71, 662-674, 2009.
- Rapp M., and F.-J. Lubken, On the nature of PMSE: Electron diffusion in the vicinity of charged particles revisited, J. Geophys. Res., 108 (D8), 8437, doi:10.1029/2002JD002857, 2003.
- Rapp M. and F.-J. Lbken, Polar mesosphere summer echoes (PMSE): review of observations and current understanding, Atmos. Chem. Phys., 4, 2601-2633, 2004.
- Rapp M. and G. E. Thomas, Modeling the microphysics of mesospheric ice particles: assessment of current capabilities and basic sensitivities, J. Atmos. Solar-Terr. Phys., 68, 2006.
- M.J. Taylor, Y. Zhao, P.-D. Pautet, M.J. Nicolls, R.L. Collins, J. Barker-Tvedtnes, C.D. Burton, B. Thurairajah, J. Reimuller, R.H. Varney, C.J. Heinselman, K. Mizutani, Coordinated optical and radar image measurements of noctilucent clouds and polar mesospheric summer echoes, J. Atmos. Solar-Terr. Phys., 71, 6-7, 675-687, 2009.
- Ulwick, J., K. Baker, M. Kelley, B. Balsley, and W. Ecklund, Comparison of Simultaneous MST Radar and Electron Density Probe Measurements During STATE, J. Geophys. Res., 93(D6), 6989-7000, 1988.